

Synthesis and Characterization of some Metal Complexes with new Ligands Derived from Amino Acid and study Biological Activity

Nora Amer Hadi¹, Murtadha Abd Ali Farhan²

^{1,2}Department of chemistry/College of education / University of Al-Qadisiyah/Iraq

Email: murtadha.ali@qu.edu.iq

Abstract

A novel 3-(3-(thiophene-2-carbonyl)thiorido)pyrazine-2-carboxylic acid (TPA) of 3-aminopyrazine-2-carboxylate and 2-thiophene carbonyl chloride, used for the synthesis of a series of new cobalt(II) mineral complexes Nickel (II), copper (II), cadmium (II), mercury (II). The mineral complexes were characterized by elemental analyzes (C.H.N.S), molar conductivity, and spectroscopic techniques: FT-IR, ¹H-NMR, ¹³C-NMR, UV-Vis, Mass spectra, and magnetic properties. The results confirmed that the ligand (TPA) behaves as a Bidentate and coordinates with the metal ion via the nitrogen atom of the amine group and an oxygen atom of the carboxyl group. The antimicrobial properties of all newly synthesized compounds were also demonstrated against the bacterial pathogenic organisms *Staphylococcus aureus* (G+) and *Escherichia coli* (G-) by the agar-well diffusion technique. These complexes are more effective against bacteria compared to the penicillin antibiotic. Cytotoxicity tests for the ligand and the mercury complex have also been performed, and in vitro studies on gastric cancer cell lines as well as normal cells (HUVEC) have shown that cancer cells absorb healthy compounds and increase their activity against cancer cells. The aim of this study describes the synthesis and characterization of the new ligand (TPA) derived from pyrazine and its metal complexes with knowing their effect on selected bacteria. And anti-cancer-activities

Keywords: Pyrazine, 2-thiophene carbonyl chloride, Transition metal complexes, biological activity.

1. Introduction

Pyrazines with a chemical formula C₄H₄N₂ are heterocyclic compounds with a characteristic smell and taste [1]. Nitrogen-containing widely distributed in plants, insects, fungi and bacteria [2-4]. Pyrazines are also very important anthropogenic compounds, especially dihydropyrazines are essential for all forms of life due to their DNA strand-breakage activity and/or by their influence on apoptosis. Along with the various classes of nitrogenous heterocyclic derivatives, pyrazines are essential components of several of pharmacologically potent compounds. Pyrazine containing drugs are widely used in the field of medicine, for example, as antineoplastic, diuretics, anti-inflammatory agents, antidepressants, neuroprotectors and anti-infective [5]. Pyrazine contains two nitrogen atoms in its aromatic ring, and it plays a vital role as intermediates for perfumes, pharmaceuticals, and agriculture chemicals and various other applications as ingredients in pesticides, insecticides, dyes and pharmaceutical compounds [6]. Pyrazines are also synthesized and degraded by several bacteria and fungi [7]. In plants or insects, naturally occurring pyrazines serve as alarming/alerting pheromones, trailpheromones, repellents in bees, and insects and moths [8].

2. Experimental

Material and reagent

All chemicals and solvents were obtained from known sources and used without further purification. Microscopic chemicals and other substances such as 3-aminopyrazine-2-carboxylic acid (99%), 2-thiophene carbonyl chloride (97%), ammonium thiocyanate (98%),

potassium hydroxide (99%), CoCl₂·6H₂O (99%), NiCl₂·6H₂O (99.9%), CuCl₂·2H₂O (99%), CdCl₂·H₂O (99%), HgCl₂ (99%), sodium hydroxide, acetone (99%), methyl sulfoxide (DMSO, 98%), Dimethylformamide (DMF, 99.9%), absolute ethanol (EtOH, 99.9), carbon tetrachloride (99%), diethyl ether (99%), methanol (MeOH, 99%), and from Sigma-Aldrich (Germany), Merck.

Physical measurements

UV-Vis spectra were recorded with a PerkinElmer spectrometer in the range 200–1100 nm and a concentration of 10–3 M. The mass spectrometry was recorded using an AB Sciex 3200 QTRAP. Primary analysis was measured using the EA 300 micro-unit (CHNS). NMR spectra were recorded using a Bruker spectrometer (500 MHz) in DMSO-d₆ (internal TMS standard). FT-IR spectra were recorded with a Shimadzu 8400S spectrophotometer using KBr discs in the (400–4000) cm range. The melting points of the ligand and its complexes were measured using a thermoelectric melting point 9300.

3. Synthesis

Synthesis of ligand (TPA) The ligand was prepared by two steps

(A)- Preparation of the (Thiophene-2-carbonyl isothiocyanate)

Mixture of 2-thiophene carbonyl chloride (3.851 ml, 26mmol) and Ammonium thiocyanate (2g, 26mmol) in (25ml) of acetone was stirred under reflux for 3 hrs. And then filtered, the filtrate was used for further reaction.

(B)-Preparation of 3-(3-(thiophene-2-carbonyl)thioureido) pyrazine-2-carboxylic acid (TPA)

From (3.654 gm) of 3-Aminopyrazine-2-carboxylic acid in (15 ml) Acetone was rapidly added to Thiophene-2-carbonyl isothiocyanate and maintaining reflux. After refluxing for 6hrs, the resulting solid was collected, washed with acetone. And recrystallization from ethanol, yield (78%) (m.p=154-157).

General method for synthesis metal complexes

Dissolved (0.6 gm, 2mmol) of the ligand (TPA) in a base alcohol solution (0.112 gm, 2mmol) of KOH in (5-8ml) of absolute ethanol and the pH is set at 7 then the solution of following metal salts, $\text{CoCl}_2 \cdot 6\text{H}_2\text{O}$ (0.237g, 1mmol) $\text{NiCl}_2 \cdot 6\text{H}_2\text{O}$ (0.237g, 1mmol), $\text{CuCl}_2 \cdot 2\text{H}_2\text{O}$ (0.170 g, 1mmol), $\text{CdCl}_2 \cdot \text{H}_2\text{O}$ (0.201g, 1mmol), and HgCl_2 (0.271 g, 1mmol) in ethanol, were added drop wise to the solution of the ligand. The precipitate formed immediately after stirring the mixture at room temperature for 3hr. The resulting precipitates were filtered off, washed with ethanol, dried and recrystallized from ethanol. Physical properties were given in Table (1).

Biological activity study (in vitro)

Antibacterial assay (in vitro)

The biological activity of the ligand (TPA) and their complexes has been tested against two types of Gram-positive bacteria (*Staphylococcus aureus*) and Gram-negative bacteria (*E. coli*) were studied. Each of these bacteria is one of the most common types of pathogenic bacteria. Biological activity solutions were prepared at a concentration of 10^{-3} mg/L each of the ligand and its metal complexes dissolved in dimethyl sulfoxide (DMSO). The culture medium was prepared according to the instructions provided by Muller-Hinton Agar Company by dissolving (38 g) of agar in one liter of distilled water. Bacteria is spread in dishes and on the surface of the food medium (Muller-Hinton agar) using (Loop full), as well as making several holes with a diameter of 6 mm in these dishes using a sterile alcohol drill. The prepared solutions were added to these holes in an amount of 0.1 ml using (Micropipette) and placed in the incubator for 24 hours at a temperature of 37°C , after which the diameter of the inhibition zone was measured in millimeters [9]. In addition, the antibiotic penicillin was tested for comparison with prepared compounds. During the experiments, bacteria and penicillin were placed in nutrient agar medium respectively. Different test microorganisms were inoculated into agar medium. The Gram method was also used to diagnose bacteria. Microbial growth was determined by measuring the area of the inhibition diameter with the help of a scale. The diameter of the inhibitory region was measured after 24 h in solvent (DMSO) for bacteria and penicillin respectively.

Cytotoxic studies-MTT assay

Cytotoxicity tests were performed on the new compound 3-(3-(thiophene-2-carbonyl) thioureido) pyrazine-2-carboxylic acid (TPA) and Hg (II). Against gastric carcinoma cell lines (MKN45) and normal endothelial cells (HUVEC). Cell lines were purchased from the Iranian Biological

Resource Center. A modified cell survival (MTT) method was applied to perform this assessment, and MTT reductase (3-[4, 5-dimethylthiazolyl]-2, 5-diphenyltetrazolium bromide) was determined using the described method. For 24 h, cells were seeded at a density of 1×10^5 cells/well in 96 clear flat plates. The medium was extracted after 24 h incubation in 5% CO_2 at 37°C , and cells were treated with sequential concentrations (25, 50, 100, 200, 400 $\mu\text{g/ml}$). After a 48 h incubation period at 37°C [10], the medium was withdrawn from the plate. Each well was then filled with 200 μl of MTT reagent (1 mg/ml) in serum-free medium. The medium was extracted 4 h later, and 200 μl (DMSO) was applied to each well. The absorbance of the MTT metabolite dissolved in DMSO was measured using a micro plate reader at a wavelength of 570 nm. Triple tests were performed at each concentration. Optical density (OD) measurement was performed on each well using a plate reader. The percentage of cell viability was calculated as (Mean OD of treated cells / Mean OD of untreated cells) \times 100. Inhibitor concentration values of 50% (IC_{50}) were measured, and IC_{50} curves were plotted using an equivalent \times dose-response.

4. Results and Discussion

Characterization of ligand (TPA) and its metal complexes

The prepared compounds were stable in air and humidity at room temperature. It was insoluble in common organic solvents such as water, carbon tetrachloride and diethyl ether, but soluble in dimethyl sulfide (DMSO), dimethylformamide (DMF), absolute ethanol (EtOH) as well as acetone.

Elemental analysis data for the Ligand and Complexes

Synthesized ligand (TPA) and its metal complexes are shown in Table (1). They are consistent with the suggested stoichiometries. The color and melting points of the synthesized ligand and its metal complexes are also shown in Table (1).

Molar conductivities of all synthesized

The molar conductivity of the metal compounds was studied in a solution of dimethyl sulfoxide (10^{-3}C) and at ambient temperature using Cond 3110 SET1 model, and the test showed that all the complexes are non-electrolytes

Infrared spectra studies of Ligand (TPA)

Spectral infrared data (KBr disk) of 3-(3-(thiophene-2-carbonyl) thioureido) pyrazine-2-carboxylic acid (TPA) (Table 2) and Fig. (1) Showed bands due to ν (NH) amide, ν (OH), ν (C=O) (amidic) and (C=S) which were observed at, (3471) cm^{-1} , (3193) cm^{-1} , (1666) cm^{-1} , (1249) cm^{-1} , respectively. While another absorption band appeared at (1689) cm^{-1} could be explained as ν (COO) asym were the ν (COO) sym was noticed (1411) cm^{-1} .

^1H -NMR studies of ligand (TPA)

The proton nuclear magnetic resonance spectrum for the

ligand (TPA) was carried out using (DMSO) as a solvent and the following peaks were detected, Figure (2) The appearance of multiple signals at δ (7.12-7.42)ppm, which is attributed to the aromatic ring of thiophene, and the appearance of several signals at δ (7.73-8.76)ppm that are due to the aromatic ring of pyrazine, and a single signal at δ (2.5)ppm which is attributed to the solvent DMSO. It also showed a single sign at δ (4.09)ppm that goes back to NH-CS, and it showed another single sign at δ (11.08)ppm that goes back to (1H,NHamine) and another single sign at (12.08)ppm which is attributed to (H,COOH) .

13C-NMR studies of ligand (TPA)

¹³C-NMR spectrum of the free ligand(TPA) in DMSO-d₆, Fig.(3) showed for following signals: signals at (128.32 -138.41) PPM For aromatic pyrazine, and signal at δ (147.9-150) ppm For aromaticThiophene, signals at δ (39.07-40.73) ppm for DMSO, where one signal at (168.3) ppm was observed for (COOH) signal at (169.7) ppm (C = O), a signal at δ (177) ppm for (C =S) .

Mass spectrometry

The mass spectrum can be used to confirm the ligand's structure as well as its complexes. Multiple peaks were seen in TPA (Fig. 4). The mass spectrum of the novel ligand (TPA) mass spectrometer displays a fundamental peak at m/z ⁺C₁₁H₈N₄O₃S₂ (308), which is attributed to the original molecular weight of the linker (TPA) (308.336), [C₁₁H₈N₄O₃S₂] (41. 33%). These data match the chemical formulas very well. Figure 4 illustrate the pattern of ligand (TPA).

Electronic spectra studies of ligand (TPA).

The ligand (TPA) spectrum showed absorption band at (264) nm (37878) cm⁻¹ and with a molar absorbance of ϵ_{max} L.mol⁻¹.cm (1431) and returns to the bundle π - π^* . And the data obtained from UV-vis spectra of the synthesized of the ligand (TPA) given in (Table3) and Fig. (5) [7]

Magnetic moment

The measured magnetic susceptibility and effective magnetic moment (μ_{eff}) values for Co(II), Ni(II), Cu(II) complexes are shown in Table (1). Ni(II), Co(II) and Cu(II), the complexes show μ_{eff} (3.95, 2.97, 1.71) B.M respectively which can be normal values for high-spin tetrahedral complexes [11].

FT-IR. Spectra

These spectra showed a remarkable difference between the bands belonging to the stretching vibration of the ν (NH) band for the amine group in the range between (3379-3440) cm⁻¹ shifted to lower frequencies by (92-31) cm⁻¹ suggesting the possibility of coordination bonding through the nitrogen atom in the amine group [12, 13]. The absorption specific to ν (COO)_{sym} was observed in the range (1450-1458) cm⁻¹ shifted to higher frequencies by (47-39) cm⁻¹ while the resulting band ν (COO)_{a sym} appeared between (1589) cm⁻¹ shifted frequencies less by (100) cm⁻¹, which indicates the coordination of the central carboxylic group [14]. The extended vibration range carbonyl group ν (C = O) and ν (C = S) either show no change or show very little in their frequencies (1650)

cm⁻¹ and (1257) cm⁻¹ respectively to indicate a lack of coordination with the metal ion, the metal-nitrogen and metal-oxygen bonds are confirmed by the presence of extended vibrations of ν (M-O) and ν (M-N) around (455–509) cm⁻¹ and (425–470) cm⁻¹, respectively. Table (2) Description of the important bands and assignment of the linker Free (TPA) and its complexes.

Electronic spectra studies

1-Spectrum of the cobalt compound [Co (TPA)₂] d⁷

The spectrum of cobalt compound (green-colored) Shows Four bands. At (35335) cm⁻¹, (28985) cm⁻¹, (15243) cm⁻¹ and (12195) cm⁻¹ which have been attributed to (283) nm with a molar absorbance of (1289) cm⁻¹ and this band attributed to (C.T), ⁴A₂ (F) → ⁴T₁ (P), ⁴A₂ (F) → ⁴T₁ (F), ⁴A₂ (F) → ⁴T₂ (F) respectively as Show in table (3). The inter electronic repulsion parameter B⁻ was calculated and found to be (509.5) cm⁻¹ and β was found to be equal (0.524) cm⁻¹ from the relation $\beta = B^- / B_0$. these parameters are accepted to Co⁺² Tetrahedral complex [15].

2- The spectrum of the nickel compound [Ni (TPA)₂] (d⁸)

The spectrum of the brown nickel compound showed an absorption band at (37174) cm⁻¹, (22988) cm⁻¹, (15037) cm⁻¹ and (10141) cm⁻¹ these bands are attributed to the (C.T), ³T₁ (F) → ³T₂ (P), ³T₁ (F) → ³A₂ (F), ³T₁ (F) → ³T₂ (F) transition respectively. the B⁻ value establish to be (506.8) cm⁻¹ while β it was found (0.486) these parameters are accepted to Tetrahedral complex for Ni⁺².

3 Spectrum of the copper compound [Cu (TPA)₂] (d⁹)

The spectrum of the copper compound (green-colored) showed three absorption band at (37735) cm⁻¹, (13227) cm⁻¹ and (11668) cm⁻¹ which due to the C.T, ²B_{1g} → ²A_{1g}, and ²B_{1g} → ²B_{2g}. respectively which was a good agreement for square Planer complexes for Cu (II) [16]

4- The spectrum of the cadmium complex [Cd (TPA)₂] d¹⁰

The spectrum of the white complex of Cd⁺² showed one band at (37453) cm⁻¹ due to C.T

5- Spectrum of a mercury compound [(Hg (TPA)₂)]

The yellow Complex of mercury Showed absorption band at (37735) cm⁻¹ which is due to C.T 5- Biological activity study (in vitro)

The biological activity of the ligand and their complexes has been tested against two types of bacteria by using the inhibition Zone method

Staphylococcuse aurous: when we comparing the results from the results in table (4) with the percentage of penicillin antibiotic inhibition we find that the ligand and copper complex showed a greater inhibition than penicillin while the cobalt Complex showed similar inhibition with penicillin and the Ni, Cd and Hg complexes showed smaller than penicillin.

Escherichia Coli: when we comparing the results with the percentage of penicillin we find the Co, Ni, Cu, and Hg complexes Showed a greater inhibition than penicillin while the Ligand showed the similar inhibition with penicillin and the Cd Complex showed the lower inhibition than penicillin antibiotic.

5. Anti-Cancer Effect

Cell lines from tumor tissues can be used to study human cancer in vitro and in vivo. According to statistics, stomach

cancer is the fourth most common type of cancer in the world, and it is the second leading cause of death from cancer. Norouzirad et al. [17] It is more common in men than women [18] and is due to the presence of infectious, environmental, and genetic factors in humans [19, 20]. Using a cell viability assay, the cytotoxic activity of ligand complex (TPA) and Hg (II) against gastric cancer cells (MKN45) and the effect of healthy cells (HUVEC) at different concentrations (25, 50, 100, 200, 400). $\mu\text{g/ml}$ (MTT assay). The ligand (TPA) prevents the death of cancer cells at a concentration of (400) $\mu\text{g/ml}$, with a cytotoxic efficacy of (96.81%). On the other hand, the Hg (II)-Complex inhibited (MKN45) to (98.12%) at a concentration of 400 $\mu\text{g/ml}$, while normal cell-cell (HUVEC) had no effect at the same concentration. Similarly, all tested compounds were most inhibited when concentrations (400 $\mu\text{g/ml}$) were incubated for 24 h, while concentrations (25 $\mu\text{g/ml}$) were at least inhibited. The selectivity index (SI), which indicates the cytotoxicity of the compound against cancer cells while it is safe against normal cells, was calculated by comparing the IC50 values for each cell line. (TPA) showed selective cytotoxicity against cancer cell lines with IC50 = 81 $\mu\text{g/ml}$, but was very healthy against normal cells with IC50 = 138 $\mu\text{g/ml}$. While the compound showed selective cytotoxicity against cancer cell lines with IC50 = 84 $\mu\text{g/ml}$ but it was very healthy against normal cells with IC50 = 131 $\mu\text{g/ml}$. Tables 5 and 6 give the viability rate values for the selected compounds after 24 h of treatment with different concentrations of (MKN45) cells and HUVEC cells and calculate the 50% inhibitory concentration (Figures 7, 8, 9 and 10). In the cytotoxicity assays performed on the

metallic compound TPA and Hg (II) using the gastric cancer cell line MKN45, and in comparison with HUVEC, and the anti-cancer efficacy evaluated the viability of the cells, it can be concluded that the bonding and metallic mercury (II) of the compound has a good and selective cytotoxic property against Gastric cancer cells MKN45

6. Conclusions

The new ligand 3-(3-(thiophene-2-carbonyl) thiorido) pyrazine-2-carboxylate (TPA) and its complexes with metal ions were prepared and characterized by analytical and spectroscopic dating. The (TPA) ligand acts binary, in coordination with the nitrogen and Oxygen atoms of the (NH) and (COO-) groups respectively as the illustration of Figure (11). Magnetic and electronic studies reveal tetrahedral Structure for all complexes expect Cu (II) complex has a square planar geometry. Biological activity assays for cell viability and cytotoxicity of ligand and Hg (II) complexes were performed using cancer cell lines (MKN45) and compared with a normal cell line (HUVEC). It can be concluded that the ligand and Hg (II) complex possess selective and cytotoxic property against the cells of the gastric cancer cell line. The biological activity of the ligand and its complexes were performed and compared with the antibiotic penicillin and the experiments showed that the ligand and all the transition compounds have good activity against bacteria.

Table 1: Color, melting point, elemental analysis and conductivity data for the synthesized TPA and metal complexes.

Compound	M.wt (gm/mol)	Color	M.P (C) Or deco.		% Yield	μ_{eff} (B.M)	Λ_{m} (ohm- cm ² mol ⁻¹) 10 ⁻³ M in DMSO	Found% (Calc.)			
								C%	H%	N%	S%
C ₁₁ H ₈ N ₄ O ₃ S ₂ (TPA)	308	orange	-157) (154)	%80	-	18	42.85 (42.74)	2.62 (3.53)	18.17 (18.31)	20.80 (20.69)	-
[Co (TPA) ₂]	673.59	green	-146) (144)	%64	3.95	13	39.23 (39.16)	2.09 (2.02)	16.64 (16.57)	19.04 (18.97)	8.75 (8.68)
[Ni(TPA) ₂]	673.35	Brown	-219) (217)	%67	2.97	5	39.24 (39.17)	2.10 (2.13)	16.14 (16.07)	19.05 (18.98)	8.72 (8.65)
[Cu(TPA) ₂]	678.20	Green	-134) (132)	%64	1.71	17	38.96 (39.89)	2.08 (2.01)	16.52 (16.45)	18.91 (18.84)	9.36 (9.29)
[Cd(TPA) ₂]	727.07	white	(243)	%72	0	11	36.34 (36.27)	1.94 (1.87)	15.41 (15.34)	17.64 (17.57)	15.46 (15.39)
[Hg(TPA) ₂]	815.25	yellow	-176) (174)	%82	0	14	32.41 (32.44)	1.73 (1.66)	13.74 (12.84)	15.73 (15.62)	24.60 (24.52)

Table (2) the characteristic bands of infrared spectra of ligand and complexes

Compound	$\nu(\text{N-H})\nu(\text{O-H})$	$\nu(\text{COO})_{\text{asymm}}$	$\nu(\text{COO})_{\text{a symm}}$	$\nu(\text{C=O})$	$\nu(\text{C=S})$	$\nu(\text{M-O})$	$\nu(\text{M-N})$
Ligand(TPA)	3471 (b) 3193(s)	1411 (m)	1689(m)	1666 (s)	1249(s)	—	—
[Co(TPA) ₂]	3409 (b)	1450 (s)	1589 (s)	1650 (w)	1257 (m)	501 (w)	439 (w)
[Ni(TPA) ₂]	3379(b)	1458(m)	1589 (m)	1650 (w)	1257 (w)	509 (w)	470 (w)
[Cu(TPA) ₂]	3425 (b)	1450(m)	1589 (s)	1650 (w)	1257 (m)	455 (w)	425 (w)
[Cd(TPA) ₂]	3440 (b)	1450 (m)	1589 (s)	1650 (m)	1257 (s)	493(w)	439 (w)
[Hg(TPA) ₂]	3425 (b)	1450 (s)	1589 (s)	1650 (m)	1257 (s)	486 (w)	447 (w)

s=strong m=medium w=weak b=broad

Table (3) Electronic spectral data of ligand (TPA) and its complexes in DMSO Solvent.

compounds	$\lambda(\text{nm})$	$\epsilon(\text{cm}^{-1})$	ABC	ϵ_{max}	Transitions
-----------	----------------------	----------------------------	-----	-------------------------	-------------

Ligand (TPA)	264	37878	1.431	1431	$\pi-\pi^*$
[Co(TPA) ₂]	283	35335	1.289	1289	C.T
	345	28985	0.500	500	4A2(F)→4T1(P) 4A2(F)→4T1(F)
	656	15243	0.150	150	4A2(F)→4T2(F)
	820	12195	0.030	30	
[Ni (TPA) ₂]	269	37174	0.962	962	C.T
	435	22988	0.185	185	3T1(F) →3T1 (P)
	665	15037	0.077	77	3T1(F) →3A2 (F)
	986	10141	0.086	86	3T1(F) →3T2(F)
[Cu (TPA) ₂]	265	37735	0.530	530	C.T
	756	13227	0.085	85	2B1g→ 2A1g
	857	11668	0.030	30	2B1g→ 2B2g
[Cd (TPA) ₂]	267	37453	1.584	1584	C.T
[Hg (TPA) ₂]	265	37735	0.709	709	C.T

C.T = Charge transfer

Table (4) Effect of ligands (TPA) and metal complexes dissolved in DMSO solvent on two types of bacteria compared to penicillin

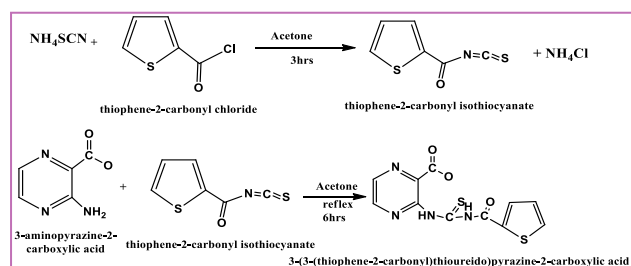
Compounds	Anti-bacterial Activity	
	Staphylococcus(+)	E.coli(-)
DMSO	-	-
Ligand (TPA)	2.3	2.0
Penicillium	2.1	2.0
[Co(TPA) ₂]	2.1	2.3
[Ni(TPA) ₂]	2.0	2.2
[Cd (TPA) ₂]	1	1.3
[Cu(TPA) ₂]	2.3	2.2
[Hg (TPA) ₂]	1	2.4

Table (5) Cytotoxicity evaluation of (TPA) versus cancer cell line (MKN45) after incubation (24 h) at (37 °C) and HUVEC cell line

Conc. $\mu\text{g.mL}^{-1}$	Ligand: (TPA)					
	Cells from the cancer line(MKN45)			Normal line cells HUVEC		
	Mean	SD	Cell% inhibition	Mean	SD	Cell% inhibition
25	89.52185	2.07599	10.47	86.44774	1.11055	13.55
50	64.34254	4.8899	35.65	76.30463	2.63039	23.69
100	47.21120	2.87184	52.78	63.00502	2.8793	36.99
200	16.33464	2.19864	83.66	40.53013	2.93012	59.46
400	3.187342	1.14568	96.81	17.71875	0.63245	82.28
IC50	81			138		

Table (6) Cytotoxicity assessment of the Hg (II) compound against a cancer cell line (MKN45) after incubation (24 h) at (37°C) and a HUVEC cell line

Conc. ($\mu\text{g/ml-1}$)	[Hg (TPA) ₂ (II)]					
	Cell from the cancer line (MKN45)			Normal Line cells Huvec		
	Cell viability		% Cell inhibition	Cell viability		% Cell inhibition
Mean	SD	Mean		SD		
25	81.23504	1.26473	18.76	95.11772	3.32735	4.88
50	66.97212	3.79419	33.02	82.53368	19.6515	17.46
100	50.79682	1.53085	49.20	57.28117	0.99522	42.71
200	21.11554	1.89534	78.88	36.02696	5.92448	63.97
400	1.872514	2.20146	98.12	15.23564	0.59761	84.76
IC50	84			131		



(Scheme-1) Preparation of (TPA)

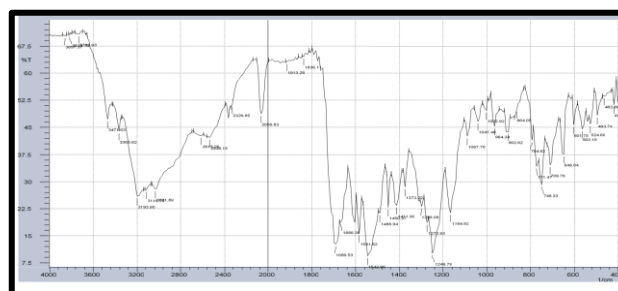


Fig. (1): Infrared spectrum of Ligand (TPA)

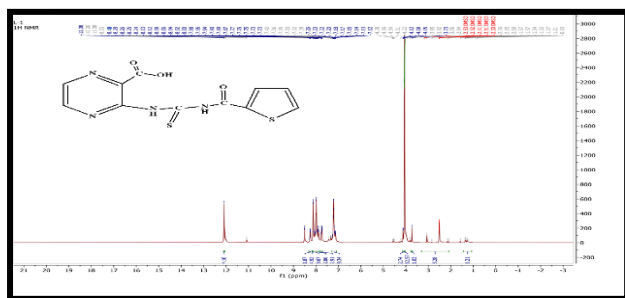


Fig. (2):¹H-NMR spectrum of ligand (TPA)

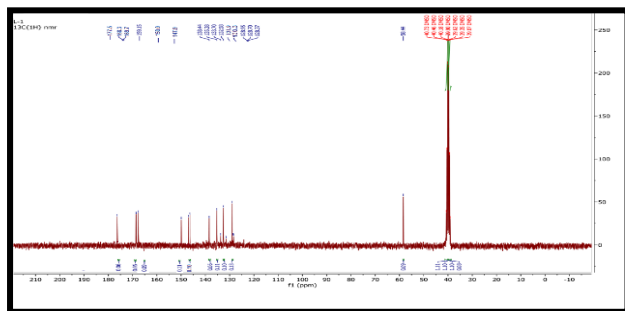


Fig. (3):¹³C-NMR spectrum of ligand (TPA)

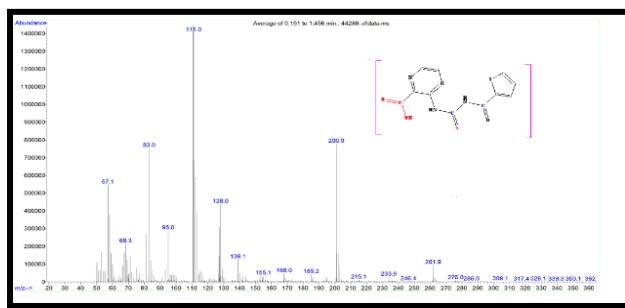


Fig. 4. Mass spectrum of ligand (TPA).

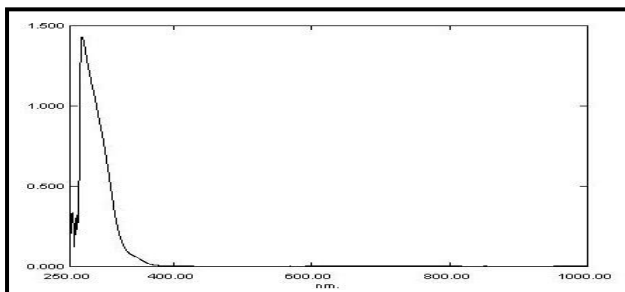


Fig. (5): Electronic spectrum of ligand (TPA)



Fig (6) the effect of TPA and its complexes on *Staphylococcus aureus* and *Escherichia coli*

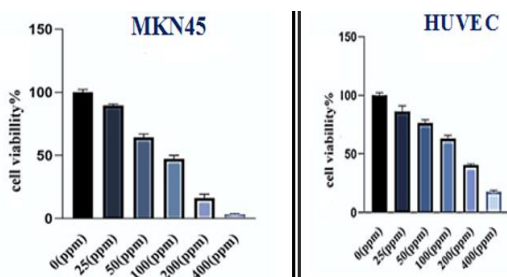


Fig. 7- % Cell viability for ligand (TPA) against cancer cells (MKN45) and the normal cells

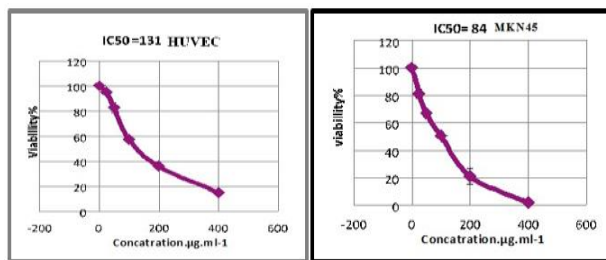


Fig. 8- IC₅₀ for ligand (TPA) in (MKN45) cell line and (HUVEC) Natural cell line.

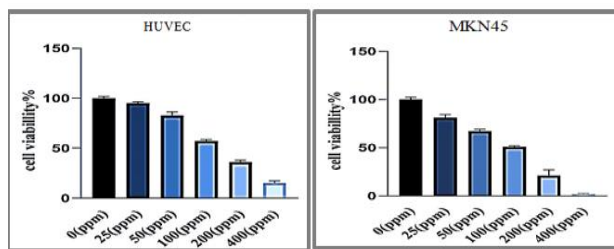


Figure 9-% cell viability of Hg (II) compound against cancerous (MKN45) cells and healthy cells

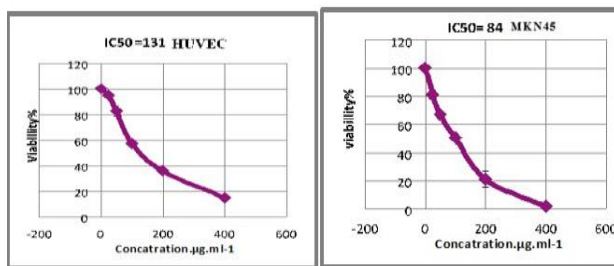


Figure 10 - Compound IC₅₀ Hg (II) in a (MKN45) and (HUVEC) cell line Normal cell line

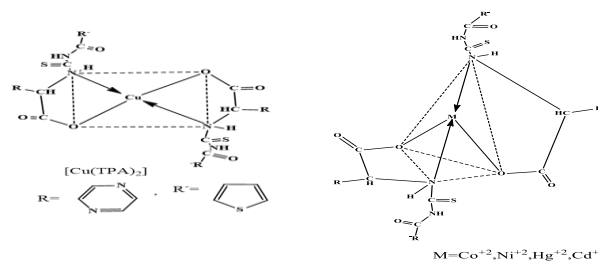


Figure. (11): The proposed chemical structure formula of the complexes.

References

- Mortzfeld FB, Hashem C, Vranková K, Winkler M, Rudroff F. Pyrazines: Synthesis and industrial application of these valuable flavor and fragrance compounds. *Biotechnology Journal*. 2020;15(11):2000064. <https://doi.org/10.1002/biot.202000064>
- Murray KE, Whitfield FB. The occurrence of 3-alkyl-2-methoxypyrazines in raw vegetables. *Journal of the Science of Food and Agriculture*. 1975;26(7):973-86. <https://doi.org/10.1002/jsfa.2740260714>
- Guilford T, NICOL C, ROTHCHILD M, MOORE BP. The biological roles of pyrazines: evidence for a warning odour function. *Biological Journal of the Linnean Society*. 1987;31(2):113-28. <https://doi.org/10.1111/j.1095-8312.1987.tb01984.x>
- Dickschat JS, Nawrath T, Thiel V, Kunze B, Müller R, Schulz S. Biosynthesis of the off-flavor 2-

methylisoborneol by the myxobacterium *Nannocystis exedens*. *Angewandte Chemie International Edition*. 2007;46(43):8287-90.

<https://doi.org/10.1002/anie.200702496>

5. Lovell KM. The Synthesis and Pharmacological Evaluation of Salvinorin A Analogues as Opioid Receptor Probes University of Kansas, 2011. Available from: <http://hdl.handle.net/1808/8148>

6. Dolezal M, Zitko J. Pyrazine derivatives: a patent review (June 2012–present). *Expert opinion on therapeutic patents*. 2015;25(1):33-47. <https://doi.org/10.1517/13543776.2014.982533>

7. Ragini M, Prashant K. A Study on Outbreak of Dengue from Bihar, India-Establishing New Foci, Attributable to Climatic Changes Ragini Mishra^{1*} and Prashant Kumar². *Journal of Public Health and Epidemiology*. 2011;3(11):489-502. Available from: <http://www.academicjournals.org/jphe>

8. Woolfson A, Rothschild M. Speculating about pyrazines. *Proceedings of the Royal Society of London Series B: Biological Sciences*. 1990;242(1304):113-9. <https://doi.org/10.1098/rspb.1990.0113>

9. Abdullah BH, Salh YM. Synthesis, characterization and biological activity of N-phenyl-N-(2-phenolyl) thiourea (PPTH) and its metal complexes of Mn (II), Co (II), Ni (II), Cu (II), Zn (II), Cd (II), Pd (II), Pt (II) and Hg (II). *Oriental Journal of Chemistry*. 2010;26(3):763.

10. Khodair AI, Alsafi MA, Nafie MS. Synthesis, molecular modeling and anti-cancer evaluation of a series of quinazoline derivatives. *Carbohydrate research*. 2019;486:107832. <https://doi.org/10.1016/j.carres.2019.107832>

11. Agostini M, Araujo G, Bakalyarov A, Balata M, Barabanov I, Baudis L, Bauer C, Bellotti E, Belogurov S, Bettini A. Final results of GERDA on the search for neutrinoless double- β decay. *Physical review letters*. 2020;125(25):252502.

12. Seenaiiah D, Venkatesh B, Padmaja A, Padmavathi V. Synthesis of some new oxazolonyl/thiazolonyl/imidazolonyl-benzoxazoles, benzothiazoles and benzimidazoles. 2013.

13. Djebbar-Sid S, Benali-Baitich O, Deloume JP. Synthesis, characterization and electrochemical behaviour of cobalt(II) and cobalt(III):O₂- complexes, respectively, with linear and tripodal tetradentate ligands derived from Schiff bases. *Journal of Molecular Structure*. 2001;569(1):121-8. [https://doi.org/10.1016/S0022-2860\(00\)00968-6](https://doi.org/10.1016/S0022-2860(00)00968-6)

14. Al-Hashimi S, Sarhan B, Salman A. Synthesis and characterization of N-acetyl-DL-tryptophan with some metal ions. *Iraq J Chem*. 2002;28:1-11.

15. Chioma F, Ekennia AC, Ibeji CU, Okafor SN, Onwudiwe DC, Osowole AA, Ujam OT. Synthesis, characterization, antimicrobial activity and DFT studies of 2-(pyrimidin-2-ylamino) naphthalene-1, 4-dione and its Mn (II), Co (II), Ni (II) and Zn (II) complexes. *Journal of Molecular Structure*. 2018;1163:455-64. <https://doi.org/10.1016/j.molstruc.2018.03.025>

16. Agrahari B, Layek S, Ganguly R, Pathak DD. Synthesis and crystal structures of salen-type Cu (ii) and Ni (ii) Schiff base complexes: application in [3+ 2]-cycloaddition and A 3-coupling reactions. *New Journal of*

Chemistry. 2018;42(16):13754-62.

<https://doi.org/10.1039/C8NJ01718B>

17. Norouzirad R, Khazaei Z, Mousavi M, Adineh HA, Hoghooghi M, Khabazkhoob M, Nirouzad F, Dorchin M, Khazaei S, Vafa MS. Epidemiology of common cancers in Dezful county, southwest of Iran. *Immunopathologia Persa*. 2017;4(1):e10.

<https://doi.org/10.15171/ipp.2018.10>

18. Bray F, Ferlay J, Soerjomataram I, Siegel RL, Torre LA, Jemal A. Global cancer statistics 2018: GLOBOCAN estimates of incidence and mortality worldwide for 36 cancers in 185 countries. *CA: a cancer journal for clinicians*. 2018;68(6):394-424.

19. Zabaleta J. Multifactorial etiology of gastric cancer. *Cancer Epigenetics*. 2012:411-35. https://doi.org/10.1007/978-1-61779-612-8_26

20. Jemal A, Bray F, Center MM, Ferlay J, Ward E, Forman D. Global cancer statistics. *CA: a cancer journal for clinicians*. 2011;61(2):69-90. <https://doi.org/10.3322/caac.20107>